Improved Single Molecule Force Spectroscopy Using Micromachined Cantilevers

Matthew S. Bull,[†,‡,∥] Ruby May A. Sullan,[†,#] Hongbin Li,[§] and Thomas T. Perkins[†,⊥,*]

[†]JILA, National Institute of Standards and Technology and University of Colorado, Boulder, Colorado 80309, United States, [‡]Department of Physics, University of Colorado, Boulder, Colorado 80309, United States, [§]Department of Chemistry, University of British Columbia, Vancouver, British Columbia V6T 1Z1, Canada, and [⊥]Department of Molecular, Cellular, and Developmental Biology, University of Colorado, Boulder, Colorado 80309, United States. [∥]Present address: Department of Applied Physics, Stanford University, Stanford, California 94305, United States. [#]Present address: Institute of Life Sciences, Université Catholique de Louvain, B-1348 Louvain-la-Neuve, Belgium.

ABSTRACT Enhancing the short-term force precision of atomic force microscopy (AFM) while maintaining excellent long-term force stability would result in improved performance across multiple AFM modalities, including single molecule force spectroscopy (SMFS). SMFS is a powerful method to probe the nanometer-scale dynamics and energetics of biomolecules (DNA, RNA, and proteins). The folding and unfolding rates of such macromolecules are sensitive to sub-pN changes in force. Recently, we demonstrated sub-pN stability over a broad bandwidth ($\Delta f = 0.01-16$ Hz) by removing the gold coating from a 100 μm long cantilever. However, this stability came at the cost of increased short-term force noise, decreased temporal response, and poor sensitivity. Here, we avoided these compromises while retaining excellent force stability by modifying a short ($L = 40$ μm) cantilever with a focused ion beam. Our process led to a ~10-fold reduction in both a cantilever's stiffness and its hydrodynamic drag near a surface. We also preserved the benefits of a highly reflective cantilever while mitigating gold-coating induced long-term drift. As a result, we extended AFM's sub-pN bandwidth by a factor of ~50 to span five decades of bandwidth ($\Delta f \approx 0.01-1000$ Hz). Measurements of mechanically stretching individual proteins showed improved force precision coupled with state-of-the-art force stability and no significant loss in temporal resolution compared to the stiffer, unmodified cantilever. Finally, these cantilevers were robust and were reused for SFMS over multiple days. Hence, we expect these responsive, yet stable, cantilevers to broadly benefit diverse AFM-based studies.

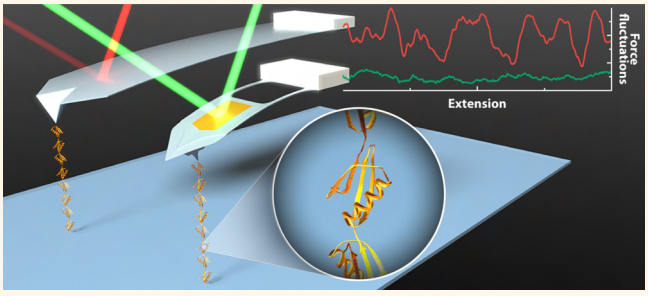

KEYWORDS: AFM · atomic force microscopy · protein folding · SMFS · focused ion beam milling · cantilever dynamics · e-beam induced deposition

Atomic force microscopy (AFM)[1] is a powerful tool in nanoscience that is having an increasing impact in biology.[2−10] AFM offers subnanometer imaging[7,11−14] in conjunction with mechanical probing of molecules[10,15−17] and cells.[18,19] The primary measurement in AFM is force (F), derived from measuring cantilever deflection. Like any measurement platform, AFM would benefit from better precision on short time scales while maintaining excellent stability over long periods. Better short-term force precision improves all AFM applications. Likewise, long-term force stability benefits multiple AFM modalities, such as imaging[20,21] and single molecule force spectroscopy (SMFS).[15] In SMFS, force stability is critical since the equilibrium between folded and unfolded states of biomolecules (proteins, RNA, and DNA) is sensitive to sub-pN changes in F.[15,22]

The path toward improved short-term force precision is well established:[23] reduce the hydrodynamic drag (β) of the cantilever. This improvement is a consequence of the fluctuation−dissipation theorem $\Delta F = (4k_BT\Delta f\beta)^{1/2}$, where ΔF is the force precision, k_BT is the thermal energy, and Δf is the bandwidth of the measurement. The primary way to reduce β is to decrease the cantilever length (L), which has led to shorter, albeit stiffer, cantilevers.[23] Stiffer cantilevers do not adversely affect force precision as long as the measured motion of the cantilever is dominated by Brownian motion (an assumption of the fluctuation−dissipation theorem).

* Address correspondence to tperkins@jila.colorado.edu.

Received for review February 21, 2014 and accepted March 26, 2014.

Published online March 26, 2014
10.1021/nn5010588

In contrast, long-term stability is limited by instrumental rather than fundamental issues. Recently, we achieved sub-pN force stability over a 100-s period (Δf = 0.01−16 Hz) in liquids by removing the gold coating of a soft (k = 6 pN/nm) cantilever. Positional precision at higher frequencies (~1 kHz) remained unchanged despite a ~10-fold reduction in reflected light.[24] The enhanced stability afforded by an uncoated cantilever revealed low-frequency instrumental drift in the optical lever arm. This drift was similar in magnitude and spectral distribution on a state-of-the-art commercial AFM (Cypher, Asylum Research) and a custom-built ultrastable AFM.[25] The drift added a fixed amount of additional positional noise per unit bandwidth, which in turn degraded the performance of stiffer cantilevers more than softer ones (Figure 1). As a result, cantilevers that are soft and long (Figure 1a) outperformed short yet stiff ones (Figure 1b) on surprisingly short time scales (~25 ms) when using two popular cantilevers, the long BioLever [k = 6 pN/nm; L = 100 μm (Olympus)] and the BioLever Mini [k = 100 pN/nm; L = 40 μm].[21]

An additional goal in SMFS is detecting small, short-lived folding intermediates.[26,27] Such detection is enhanced by improved short-term force precision and fast response of the cantilever to an abrupt change in F. Unfortunately, the long BioLevers that provide the best force stability suffer from relatively poor temporal resolution due to their increased β and decreased k. This reduced temporal resolution, coupled with decreased short-term force precision, hinders their application in such SMFS studies.

Thus, at the moment, choosing the appropriate cantilever for a particular application requires a compromise. This choice arises from the basic scaling relation governing cantilever stiffness: $k \propto wT^3/L^3$, where w is the width of a rectangular cantilever, and T is its thickness. Reductions in β arising from decreased L necessarily lead to increased k. As a result, a user can have a stiff, low-force noise cantilever at the cost of reduced long-term stability. Alternatively, one can get state-of-the-art long-term force stability, but with increased force noise per unit bandwidth and reduced temporal resolution. For applications that require high reflectivity, gold-coated cantilevers lead to particularly poor long-term force stability.

We avoided these compromises by modifying a short (L = 40 μm) commercial cantilever using a focused ion-beam (FIB) (Figure 1c). Micromachining of cantilevers with a FIB has led to significant drops in both k and β.[28,29] However, these benefits have not yet been exploited in biophysical and nanoscience research applications using the traditional optical lever arm detection available on commercial AFMs.

In this paper, we developed an efficient protocol for enhancing the spatial-temporal measurement limits of a widely used commercial cantilever (BioLever Mini)

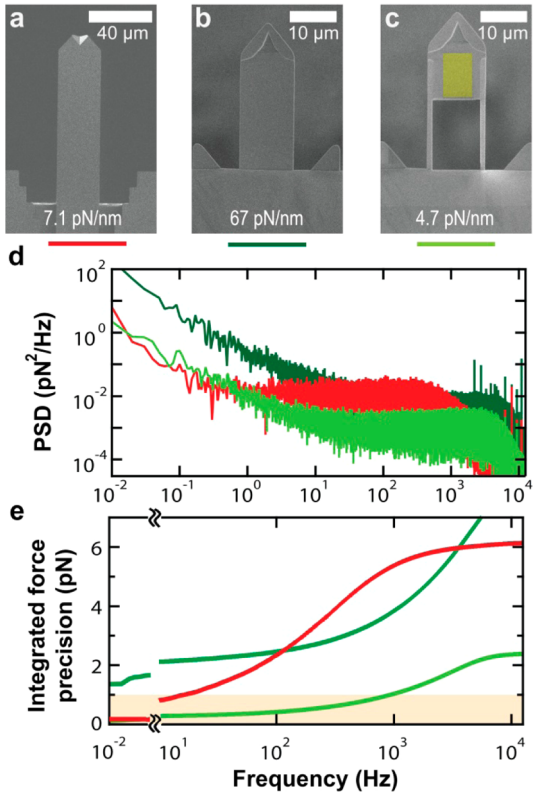

Figure 1. Micromachined cantilevers show improved performance. SEM images of (a) an uncoated long BioLever (L = 100 μm), (b) an uncoated BioLever Mini (L = 40 μm), and (c) a FIB-modified BioLever Mini that has a transparent glass capping layer protecting an underlying gold patch at the end of the cantilever. Each cantilever's measured spring constant is indicated. (d) The averaged force power spectral density (PSD) as a function of frequency of each cantilever in liquid is shown when the cantilever was 50 nm over the surface. The color of the curve is associated with the line immediately below each cantilever's image in (a−c). (e) Integrated force noise for each cantilever shown as a function of frequency. The sub-pN regime is shaded orange. The gold patch in panel (c) is false colored for visual clarity.

(Figure 2) and explored its application in precision protein-unfolding experiments. Removing a large section of the cantilever led to a 10-fold reduction in the hydrodynamic drag, improving short-term force precision. We simultaneously achieved a 10-fold reduction in stiffness by thinning the remaining beams, facilitating excellent long-term force stability. A transparent capping layer patterned at the end of the cantilever allowed us to retain a gold-coated cantilever's high reflectivity while removing the gold from the rest of the cantilever for improved force stability. As a result, we extended the AFM's sub-pN bandwidth by a factor of ~50 to span a total of five decades of bandwidth ($\Delta f \approx$ 0.01−1000 Hz). Our FIB-modified cantilevers could be reused in SMFS assays over multiple days, increasing their cost effectiveness. In protein-based SMFS assays, we demonstrated improved short-term force precision coupled with state-of-the-art force stability. Moreover, these soft, but short, cantilevers suffered no significant loss in temporal resolution when measuring abrupt

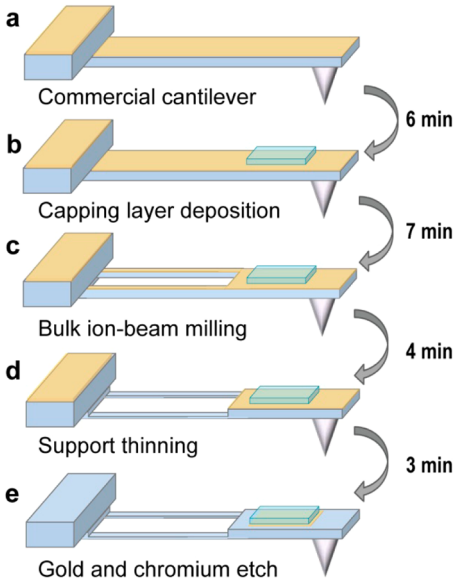

Figure 2. A four-step protocol for micromachined cantilevers. (a) A commercially available cantilever (Biolever Mini) is selected for modification. (b) A glass-like capping layer is deposited *via* e-beam-induced deposition. (c) A focused ion beam (FIB) cuts out the central region of the cantilever. (d) Using a defocused beam, the narrow cantilever supports are thinned. (e) Two 40 s wet etches remove all of the unprotected gold and chromium to improve low-frequency performance.

transitions due to protein unfolding, as compared to the stiffer unmodified cantilever. Overall, this combination of improved force precision without loss of temporal resolution, force stability, or sensitivity opens the door to many exciting AFM-based studies of short-lived nanoscale events, including single-molecule studies of protein folding over extended periods (100 s), a duration 25-fold longer than previous equilibrium AFM studies.[15]

RESULTS AND DISCUSSION

Our goal was to improve the performance of AFM in a broad range of biophysical and nanoscience applications while retaining a high-level of usability at an affordable cost. Ease of use was achieved, in part, by preserving a small gold-coated region on the back of the cantilever while minimizing drift induced by the gold coating. The long-term force stability, which was limited by instrumental drift in the optical lever arm, was achieved by lowering k. Short-term force precision was limited by the hydrodynamic drag, a consequence of the fluctuation−dissipation theorem. Thus, we sought to simultaneously reduce k and β while preserving the high reflectivity in an efficient process.

Highly Reflective Micromachined Cantilevers. In prior work, we showed that removing a cantilever's gold coating enabled sub-pN force precision over a broad bandwidth, but also led to a 10-fold loss in reflectivity.[24] The decreased optical signal did not adversely affect positional precision on soft cantilevers (k = 6 pN/nm) at ~1 kHz on a state-of-the-art commercial AFM, but did decrease the usability of uncoated cantilevers. For example, they showed more pronounced interference-induced oscillations in the cantilever signal,[21] particularly on gold-coated substrates commonly used in single-molecule[30,31] and nanoscience applications.[32,33] Reduced reflectivity is also expected to adversely impact performance when using stiffer cantilevers at higher frequencies (>10 kHz) and on older instruments.

A cantilever is most sensitive to the adverse effects of gold at the region of highest curvature, the junction between the base of the cantilever and the chip on which it is mounted. Previously, researchers have created spatial patterning of gold near the end of a cantilever by FIB milling off a cantilever's gold coating.[34] Similarly, we fully removed the gold and underlying chromium layer using an FIB. These cantilevers exhibited improved low-frequency performance. However, we consistently observed better low-frequency performance by using a wet chemical etch.

To preserve reflectivity while also achieving excellent long-term stability, we developed an e-beam patterned capping layer to preserve a small, well-defined section of gold on the back side of the cantilever. This capping layer protected the cantilever's gold coating during a subsequent wet etch that removed both the gold and chromium from the rest of the cantilever. Importantly, the capping layer was made from tetraethyl orthosilicate (TEOS), a glass-like substance that is optically transparent (see Methods). As a result, the 30−40 nm thick TEOS layer did not adversely affect optical-lever-arm detection. Fully FIB-modified cantilevers, as shown in Figure 1c, retained excellent sensitivity (~15−20 nm/V) when using the Cypher's standard (not small) spot size module in comparison to an uncoated BioLever Mini (~130 nm/V) and showed a minimal (25%) loss in the optical signal. If necessary, larger reflective regions can be fabricated by extending the TEOS patch over the full area of the end of the cantilever.

Reducing Cantilever Stiffness. We initially reduced k by removing a larger rectangular area ($20 \times 14\ \mu m^2$) from the base of a BioLever Mini. The starting width of the cantilever was ~16 μm, and our modification left two 1 μm wide supporting beams (Figure 1c). These supports were positioned at the edge of cantilever to retain torsional stiffness. Finite-element modeling and the linear scaling of k with w suggested an 8-fold reduction in w should lead to an 8-fold reduction in k. Experimentally, we measured a ~6-fold reduction. Additional reduction in k can be made by further narrowing of the support beams; we have made beams as narrow as 600 nm, but this was technically demanding. Instead, we focused on reducing the thickness of the cantilever, because $k \sim T^3$. A defocused FIB scanned along the long axis of the beam reduced the thickness from ~170 to ~120 nm. This thinning

resulted in a total reduction in k by a factor of ~10 [9.4 ± 0.9 (N = 10)]. For the particular cantilever shown in Figure 1c, the unmodified k was initially 54 pN/nm and reduced to 4.7 pN/nm, a 12-fold reduction. Further thinning of the cantilever is possible, though it resulted in a rapidly increasing fraction of cantilevers breaking during such thinning. Overall, this micromachining process generated the desired short, but soft, cantilevers.

Characterizing the Performance of Micromachined Cantilevers. The dominant noise sources in AFM-based biophysical measurements (*i.e.*, Brownian motion, instrumental noise in the optical lever arm, and metallization-induced drift of the cantilever) also affect a simpler measurement: the zero force position (z_0) of the cantilever. Our initial characterization of the FIB-modified cantilevers focused on this simpler measurement. Moreover, we performed this characterization 50 nm over the surface, since most AFM-based assays are done in close proximity to a surface. This proximity increases a cantilever's hydrodynamic damping, a phenomenon called squeezed-film damping in AFM[28] and conceptually similar to Faxen's law in optical-trapping studies.[35] Increased damping near a surface degrades short-term force precision.[36]

Characterizing cantilever motion as a function of frequency (f) allows for easy identification of two regimes: thermal- and instrumentation-limited performance. The force power spectral density (PSD) was calculated from a set of five 100 s records for each cantilever (Figure 1d) (Methods). The thermally limited regime is at higher f, where the PSD is flat as a function of f and then starts to fall off at a characteristic roll-off frequency analogous to the PSD of optically trapped beads.[35] The instrumentation-limited regime is seen at lower f, where the PSD increases as f decreases. The crossover between these two regimes differs for the three cantilevers studied.

The two uncoated commercial cantilevers show better performance in different regimes.[24] The BioLever Mini outperformed the long BioLever in the thermally limited regime (higher f) because of its lower hydrodynamic drag relative to the long BioLever. On the other hand, the long BioLever outperformed the BioLever Mini in the instrumentation-limited regime (lower f) because of its lower stiffness. As a result, the optimum cantilever depends on duration of the experiments, and the crossover between the two regimes happens at surprisingly short times (~25 ms).[21]

Our micromachined cantilever combines the advantages of the two different cantilevers and improves upon them. By decreasing the stiffness of a BioLever Mini, the modified cantilever has a low-frequency performance equal to an uncoated long BioLever. This translates into excellent long-term force stability. In the thermally limited regime at higher f, the modified cantilever has a lower PSD than the BioLever Mini and, hence, better short-term force precision. The degree of improvement can be quantified by taking the ratio of the flat sections of the PSD for the two cantilevers. This analysis shows a 3.5-fold improvement, despite the modified cantilever being 14-fold less stiff.

The kinetics of folding and unfolding of molecules are sensitive to the total applied force. Thus, a key metric is the force stability over the full duration of the experiment. Current state-of-the-art AFM experiments measure the equilibrium folding and unfolding of a protein over a few seconds.[15] In contrast, equilibrium assays with dual-beam optical-trapping experiments may last tens to hundreds of seconds.[37,38] To span both current and future AFM experiments, we calculated the integrated force noise over a 100-s period, similar to our prior work.[24] The benefits of micromachined cantilevers are immediately obvious (Figure 1e). Their reduced k allows them to have the long-term force stability equivalent to a long BioLever. Yet, their reduced β allows the integrated force noise remained at sub-pN levels to 930 Hz, a significantly higher f than the long BioLever (16 Hz). Hence, the FIB-modified cantilevers exhibited a ~50-fold increase in sub-pN bandwidth to span five decades of bandwidth ($\Delta f \approx 0.01-1000$ Hz).

Comparison with Highly Reflective Cantilevers. For applications and instruments that require high reflectivity, it is useful to compare our FIB-modified cantilevers with two traditional gold-coated cantilevers (the long BioLever and the BioLever Mini). A useful metric to characterize performance over varying averaging times is the Allan variance[39] (see Methods). The Allan variance at a given averaging time represents the averaged force noise over that time interval. More broadly, a plot of the Allan variance is another metric to characterize the crossover between thermally limited and instrumentation-limited performance.[40] We computed the Allan variance for isolated cantilevers held 50-nm over the surface (Figure 3). The Allan variance initially increases, suggesting worse performance at longer times. However, this is an artifact due to correlated motion of the cantilever at short time scales;[21] this portion of the curve is de-emphasized by plotting it in gray. Over longer averaging times, the force noise drops with a slope consistent with averaging Brownian motion. At sufficiently long times, the Allan variance for all three cantilevers deviates from this slope. At this point, instrumental noise starts to contribute and eventually dominates the average force noise on the longest time scales

Comparison of the Allan variance for the three highly reflective cantilevers immediately shows the benefit of the micromachined cantilevers. Over all time scales investigated (0.00005−50 s), the modified cantilever outperforms both commercial cantilevers. This performance improvement is particularly pronounced

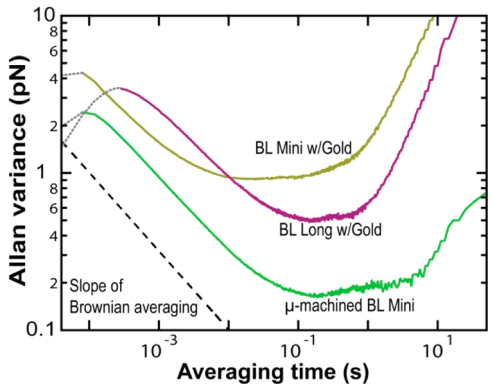

Figure 3. Comparing the performance of three different gold-coated cantilevers. Allan variance, a measure of precision over a given averaging time, was calculated from a 100 s trace measured 50 nm over a surface for a gold-coated BioLever (BL) Mini (k = 79 pN/nm, *gold*), a gold coated long BioLever (k = 5.0 pN/nm, *purple*), and a FIB-modified BL Mini (k = 5.1 pN/nm, *lt. green*). The gray dashed line is a reference with a slope consistent with averaging Brownian motion. The micromachined cantilever significantly outperformed both commercial cantilevers, particularly on time scales longer than 0.1 s. On these time scales, the detrimental effects of gold on force stability are particularly pronounced. We note that at the very shortest times when the motion of the cantilever is correlated, the Allan variance yields misleading results on force precision, and this region of the trace is de-emphasized using a dotted gray line.

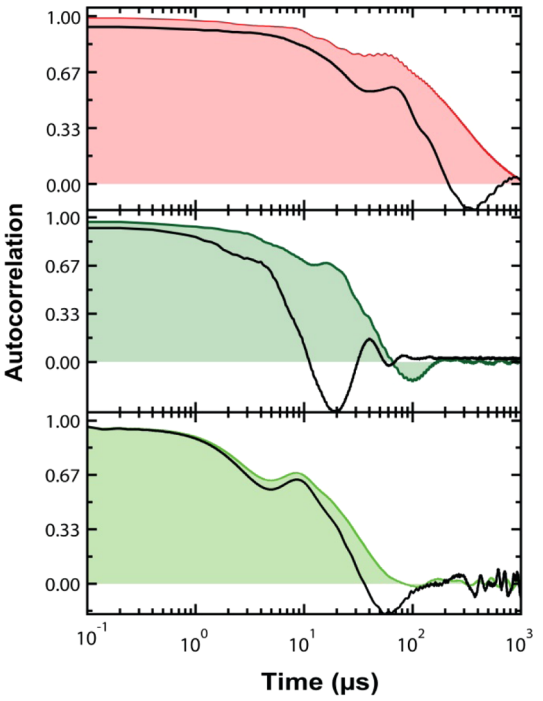

Figure 4. Temporal response of cantilevers in liquid near (50 nm) and far (~50 μm) from the surface. The autocorrelation of thermal motion as a function of time is plotted for cantilevers near (*colored*) and far (*black*) from the surface for an uncoated long BioLever (top panel), an uncoated BioLever Mini (middle panel), and a modified BioLever Mini (bottom panel). A characteristic time for each cantilever is determined by the e^{-1} point in the autocorrelation. A negative autocorrelation indicates the cantilever was slightly underdampled (Q > 1). The data show all three cantilevers with a longer correlation time and reduced Q near surfaces, consistent with increased hydrodynamic drag due to the proximity of a surface. However, the modified BioLever Mini shows less increase (85%) in its characteristic response times in comparison to the other two cantilevers (250% and 300% for the long Biolever and BioLever Mini, respectively). The characteristic response times far and near from the surface are 105 and 370 μs for the long BioLever, 8 and 31 μs for the BioLever Mini and 20 and 37 μs for the modified BioLever Mini. The stiffness for the three cantilevers are 6.4, 69, and 5.3 pN/nm for the long BioLever, the BioLever Mini, and the modified BioLever Mini, respectively.

on longer time scales (0.1−50 s) because of the detrimental effect of gold on force stability.[24] Note that performance of a gold-coated BioLever Mini deviates from thermally limited performance at unexpectedly short time scales (~1 ms). Hence, in applications requiring high reflectivity, our modified BioLever Mini shows superior performance on both short and long time scales.

Reduced Hydrodynamic Damping. For many biophysicists familiar with low Reynolds number hydrodynamics, a substantial reduction in β arising from a change in the shape, but not the longest length, of an object is not obvious.[41] On the other hand, experts in cantilever dynamics may be familiar with prior success in reducing β by FIB modification of a cantilever's shape.[28,29] To quantify β, our first metric is based on a classic result for an overdamped oscillator:[41] $\beta = k \times \tau$, where τ is the characteristic relaxation time. Our experimental definition of τ is when the autocorrelation dropped to 37% (e^{-1}) of its starting value. We measured the autocorrelation for each cantilever near and far from the surface (Figure 4). The resulting autocorrelations were not a simple monotonic function but show a slight shoulder and, for some cantilevers, ringing. The shoulder is consistent with the first harmonic of the cantilever. The ringing, or slightly negative values at longer delay times, is consistent with Q > 1. We note that the increased β near a surface suppressed such ringing for both the long BioLever and the modified BioLever Mini. Suppression of ringing is advantageous in most SMFS applications, since a sinusoidal variation of F complicates interpretation of a thermally activated process, such as protein unfolding.

We first analyzed the change in β when the cantilever is far from a surface on the basis of the ratio of β between an unmodified BioLever Mini and FIB-modified cantilever. This analysis yields a 6-fold reduction in β, a significant change considering the length of cantilever was not altered. We caution that this is a qualitative rather than a quantitative result. The calculation of β assumes overdamped motion, a valid assumption for the modified, but not the unmodified, BioLever Mini when far from the surface. Nonetheless, this result suggests a substantial reduction in β for the modified cantilevers.

The more relevant result is β when the cantilever is 50 nm over a surface. For the unmodified long BioLever and BioLever Mini, analysis of the autocorrelation time

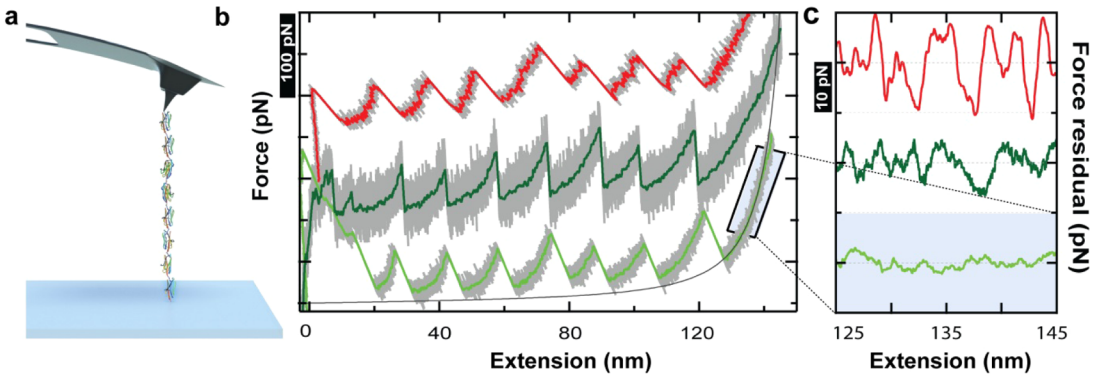

Figure 5. Improved single molecule force spectroscopy with FIB-modified cantilevers. (a) Cartoon of assay where eight domains of a polyprotein are mechanically stretched by an AFM. (b) Force−extension records of mechanically unfolding a polyprotein of NuG2 at 400 nm/s with the long BioLever (*red*), the BioLever Mini (*dark green*), and the micromachined BioLever Mini (*lt. green*). High-bandwidth data (50 kHz, *gray*) and smoothed data (1 kHz, *colored*) are shown. A worm-like-chain (WLC) model (*black line*) well describes the stretching of the protein in one state (see also Figure S2a, SI). (c) Plot of residual force fluctuations after fitting a 20 nm section of the 1 kHz data to a WLC model. The standard deviations of these fluctuations are 4.1, 2.6, and 1.2 pN, using the same color scheme as in (b). Traces displaced vertically for clarity.

shows a 250 and 300% increase in τ and, therefore, β, respectively. In contrast, the increase in τ for the FIB-modified cantilever was only 85%. Hence, the large central cutout of the cantilever not only reduced β far from the surface, it also significantly reduced the effect of increased β near surfaces due to the squeezed film damping, similar to prior results.[28] To compare β for a modified and a standard BioLever Mini at 50 nm over the surface, we computed the ratio of β for the two cantilevers. This analysis shows a 12-fold reduction in β for the individual cantilever shown in Figure 4. This ratio is computed from records of the same individual cantilever before and after modification. The resulting average reduction in β for multiple cantilevers was 10 ± 1 ($N = 5$). We note that both cantilevers showed an absence of significant ringing in their autocorrelation function close to a surface (Figure 4). Hence, we expect that this ratio in β to be a quantitative result.

For completeness, we also measured β using a generalization of Stokes drag: $F = \beta \times v$.[41] To do so, we started with the cantilever touching the surface and moved it to 100 nm above the surface at increasing v while measuring cantilever deflection. A plot of $F-v$ for all three types of cantilevers studied showed a linear relationship (Figure S1, Suppporting Information (SI)). The slope of this line yields an independent estimate of β. The ratio of the slopes for the FIB-modified and a standard BioLever Mini is ~5. However, we note that this is not our preferred quantitative determination of β because of the dependence of β with height over the surface and the short measurement time [1.6 ms (= 100 nm/60 μm/s)]. Summarizing two different analyses show a significant reduction in β near a surface, the relevant regime for most AFM-based assays. Future work can build upon our analysis for a more detailed examination of β near a surface.

Improved Single Molecule Force Spectroscopy. To demonstrate the benefit of micromachined cantilevers for real-world applications, we performed a common AFM-based single-molecule assay, mechanical unfolding of an individual protein (Figure 5a). The studied protein consisted of 8 identical repeats of NuG2, a computationally derived fast-folding variant of the protein G B1 domain (GB1).[42] As is typical for these studies, the cantilever was retracted at a constant v (400 nm/s) while measuring the resulting F. We recorded the data at 50 kHz and analyzed records that showed eight ruptures. The resulting traces showed the classic sawtooth pattern for all three cantilever types studied (Figure 5b).

Visual inspection of Figure 5b shows a dramatic improvement in the quality of the data by using a FIB-modified cantilever over either of the two commercial cantilevers, particularly when looking at the records smoothed to 1 kHz. We illustrate this improvement by analyzing the fluctuations in F. To do so, we fit a short (20 nm) section of the smoothed force−extension record to a worm-like chain (WLC) model and plotted the residual fluctuations in F (Figure 5c). The RMS fluctuations around mean position were 1.2 pN for the FIB-modified BioLever while the unmodified BioLever mini and long BioLever showed 2.6 and 4.1 pN, respectively. This reduction in force fluctuations for the modified BioLever Mini in a biophysical assay confirms a significantly reduced β. More generally, these force−extension curves were well fit by a WLC model (Figure S2a, SI) and illustrate the types of improvements afforded by micromachined cantilevers in a common AFM-based assay that requires short-term force precision.

A 10-fold reduction in β improves SMFS in another manner; it decreases the hydrodynamic force applied to the cantilever when collecting force−extension data by retracting the cantilever through a fluid. If unaccounted for, this force corrupts the classic sawtooth force−extension curve (Figure 5b), even at velocities as

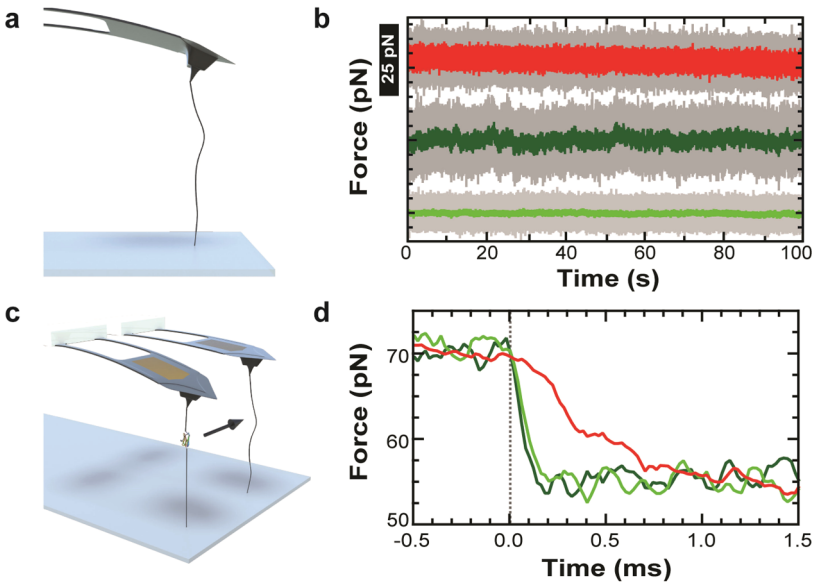

Figure 6. Micromachined cantilever shows improved performance while stretching a protein. (a) Schematic of the experiment showing a protein stretched at constant extension. (b) Force-*versus*-time records for three different cantilevers stretching a protein to $F \approx 50$ pN while the stage position was held fixed. High-bandwidth data (50 kHz, *gray*) and smoothed data (1 kHz, *colored*) are shown. Traces displaced for clarity. The standard deviation for the 1 kHz data was 5.2, 3.2, and 1.0 pN, for the long BioLever (*red*), BioLever Mini (*dark green*), and the FIB-modified BioLever Mini (*lt. green*), respectively. The stiffnesses for the three cantilevers were 4.4, 74, and 5.9 pN/nm in the same order. (c) Schematic showing the abrupt unfolding of a protein observed while holding the cantilever at constant height over the surface. (d) Averaged force-*versus*-time records show the step response function of the different cantilevers. The characteristic times for the three cantilevers were 450 (±40), 53 (±16), and 76 (±18) μs for a long BioLever (*red*), a BioLever Mini (*dark green*), and a modified BioLever Mini (*lt. green*), respectively. Note, the smoother appearance of the long BioLever record relative to the two other cantilevers is an artificial result arising from plotting data at 50 kHz where the individual points are not statistically independent (see also Figure 3).

low as a few μm/s when using standard cantilevers.[43,44] Reduction in hydrodynamic force also facilitates SMFS at very high pulling velocities ($v = 0.5-5$ mm/s), which has recently opened the door for direct comparison between SMFS data and molecular dynamics simulations.[45]

Cantilevers with reduced β can improve imaging applications as well, in particular nanoscale mapping of the mechanical properties of materials.[46] In such experiments, an array of force–distance curves is measured at every x–y point, a so-called force–volume or force–distance map. This process is usually very slow. Recently, software and hardware enhancements have led to rapid nanomechanical investigations of cells[47] and membrane proteins with molecular[48] and submolecular resolution.[49] Rapid force-volume imaging is commercially available [*e.g.*, PeakForce Tapping (Bruker)]. The quality and the speed of such experiments could be improved by using cantilevers that have both reduced k and β.

Enhanced Sub-pN Precision and Stability in Surface-Anchored Biophysical Assay. Equilibrium studies of macromolecular folding need excellent short-term force precision coupled with long-term stability. To probe long-term stability in a single-molecule assay, we first mechanically unfolded a polyprotein of NuG2 to its full extension and then lowered the cantilever until $F = 50$ pN. This F prevented refolding while allowing for the acquisition of a 100 s trace recorded at a stationary stage position (Figure 6a). The resulting data showed excellent force stability (Figure 6b) when the instrument had been allowed to settle for 1–2 h after cantilever mounting. Quantitatively, the FIB-modified cantilever showed an excellent combination of force precision and force stability with an integrated force noise of 1.1 pN over five decades of bandwidth ($\Delta f =$ 0.01–1000 Hz). The same metric yielded 2.4 and 5.2 pN for the BioLever Mini and the long BioLever, respectively. We note that this level of performance relied upon the stability of our commercial AFM; neither F nor the tip–sample separation[25] was actively stabilized. Rather, a closed-loop piezo-electric stage was used to maintain the stage position, as is typical in such assays. Different instruments will yield different results. However, the critical point is that micromachined cantilevers maintained essentially the same force stability in a protein-based assay as for an isolated cantilever (Figure 1e). As a result, our ~50-fold improvement in bandwidth for sub-pN force precision is preserved in a biophysical assay even when the cantilever is anchored to a surface through the molecule under study.

These long records of protein extension also allowed us to explore short-term force precision in an assay analogous to equilibrium studies of protein folding and unfolding.[15] As discussed above, better short-term force precision enables more robust detection of transiently populated states during SMFS studies of protein folding.[26,27] A plot of the Allan variance

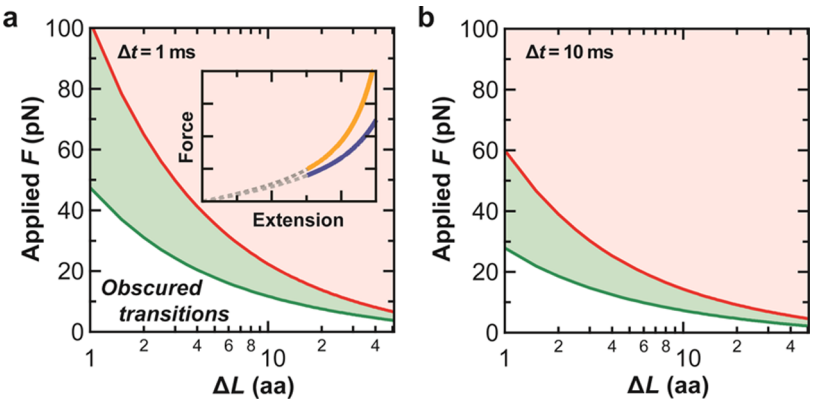

Figure 7. Analyzing the limits for detection of short-lived events as a function of force and event duration (Δt). (a, inset) Force–extension record for stretching a polyprotein consisting of three (*orange*) and four (*blue*) unfolded NuG2 domains. The two curves were considered distinguishable, and therefore color coded, when they were separated by twice the standard deviation in the force noise in data smoothed over the specified event time. (a) Plot of applied force *versus* resolvable change in contour length (ΔL) for a 1 ms event for the FIB-modified cantilever (*green*) and the uncoated long BioLever (*red*), the two cantilevers with necessary force stability for long equilibrium experiments. (b) Same as in panel (a) but analyzed assuming a 10 ms event. Note that the FIB-modified cantilever can resolve a smaller change in ΔL during a 1 ms event than the long BioLever can in a 10 ms event.

for the isolated modified BioLever *versus* one pulling on a protein at constant extension shows similar performance (Figure S3, SI). This analysis shows that improvements in short-term force precision afforded by the micromachined cantilever in a biophysical assay continued to nearly match that of an isolated cantilever.

Sensitive but Responsive in Protein-Unfolding Studies. Improved protein folding and unfolding studies rely not only on force precision, but also on cantilevers that respond rapidly to an abrupt change in applied F. While short-term force noise is governed by β, the mechanical response time is given by $\tau = \beta/k$ in the overdamped limit. Thus, in general, softer cantilevers are less responsive at fixed β.

We used the abrupt opening of a protein to directly measure the response function of the cantilever (Figure 6c). Our protocol was similar to the protein-pulling protocol used for Figure 5. In this revised assay, we selected for a full-length construct, lowered the extension until $F \approx 10$ pN and then kept the stage at a constant position. After waiting 5 s, the extension was rapidly increased until $F \approx 70$ pN. The resulting data was then recorded at high bandwidth (50 kHz) for the next 3 s. If the tether did not break, the force was returned to 10 pN for 5 s and the process repeated. To improve the signal-to-noise ratio, we averaged several unfolding trajectories ($N = 6$). The resulting data showed an approximately exponential drop in F due to the abrupt unfolding of a protein (Figure 6d). The characteristic times for a normal BioLever Mini and a modified BioLever Mini were 53 (±16) and 76 (±18) μs, respectively. These times were significantly faster than the 450 (±40) μs measured for a long BioLever. Thus, our soft cantilevers facilitate equilibrium studies because of their long-term force stability, while their reduced β allows them to be responsive in detecting short-lived events.

Improved Detection of Short-Lived States. Short-term force precision facilitates many nanoscience applications. For instance, better short-term force precision enables more robust detection of transiently populated states during SMFS studies of protein folding. Such transient states may last only 1 ms or less in equilibrium studies.[37] Transiently populated unfolding intermediates are also observed while mechanically unfolding proteins[26,27] and RNA[22] at a constant velocity. To analyze the limits in detecting the folding and unfolding of proteins in an equilibrium assay, we calculated the smallest protein-unfolding event that could be resolved when using the two cantilevers that show the necessary long-term force stability for such an assay, the modified BioLever Mini and the uncoated long BioLever. A change in L was considered detectable if two states, defined by WLC curves, were separated by twice the standard deviation in the data in a given time interval where the initial L was 53 nm (Figure 7a, inset).

Detection of short-lived events depends on the applied force and the duration of the event. We used 10 pN as a representative force, since equilibrium folding between states for a variety of biomolecules is seen at 5–12 pN.[15,37,38,50] We initially used the standard deviation of a cantilever's motion when smoothed over a 1 ms period. This analysis showed that our modified cantilever could detect a $\Delta L = 13$ amino acids [aa (1 aa = 0.36 nm)] in 1 ms (Figure 7a). In comparison, the same analysis yielded $\Delta L = 31$ aa for an uncoated long BioLever. Longer events allow for more averaging of Brownian motion, and therefore a smaller ΔL is resolvable. When a 10 ms event was analyzed, the micromachined cantilever and the long BioLever could detect a ΔL of 6 and 18 aa, respectively (Figure 7b). We note this analysis is based solely on short-term RMS noise and does not take into account

the comparatively slow mechanical relaxation of the long BioLever (0.45 ms), which makes a 1 ms event even more challenging to resolve.

Dynamic experiments also show folding intermediates[26,27] and benefit from improved detection of short-lived events. Unfolding forces of >50 pN at pulling rates of 300−500 nm/s are common.[26,27] In this regime of ∼2−3 ms/nm at F = 50 pN, our analysis suggests that detecting even a single amino acid change (ΔL = 1 aa) is possible with FIB-modified cantilevers.

In summary, our modified cantilevers excel at resolving small changes in ΔL over short periods. Indeed, they can resolve a smaller ΔL in 1 ms than an uncoated long BioLever can over 10 ms without sacrificing the force stability of the uncoated cantilever. Moreover, these modified cantilevers respond more quickly and have a high reflectivity. Overall, we expect these cantilevers will aid both equilibrium and dynamic studies of protein folding by AFM.

Cost, Usability, and Limitations. Our FIB-modified cantilevers are not too costly for routine use. After an extended research and development phase, our marginal cost for making these cantilevers in batches of 9 is ∼$30/ea at a typical academic rate for using an FIB ($75/h) operated by an undergraduate research assistant ($12/h). This marginal cost is about two-thirds the cost of a BioLever Mini or one-third of the cost of a BioLever Fast. Thus, for a relatively modest increase in cost per cantilever, one gets a dramatic improvement in performance over a broad bandwidth.

Perhaps more important than the marginal cost is that we reused FIB-modified cantilevers in SMFS applications over multiple days (Figure S2b, SI). Unlike imaging applications, SMFS does not require a particularly sharp tip. After cleaning, the reused cantilever showed no change in stiffness or loss in performance, increasing the return on investment in fabricating them.

Like many soft cantilevers, these modified cantilevers sometimes folded when immersed into liquid. However, given sufficient time (∼5 min), they typically unfolded. If the cantilever remained folded, dewetting/rewetting a few times typically induced unfolding. In cases where rewetting was unsuccessful, the cantilevers were induced to unfold by briefly dipping them in ethyl alcohol. In our experience, this behavior is quite comparable to standard long BioLevers. For comparison, we have also FIB-modified short BioLevers [L = 60 μm; k = 30 pN/nm (unmodified values)]. Unfortunately, these cantilevers rarely unfolded, making them a poor choice for routine use.

Our micromachined cantilevers showed long-term stability equal to an uncoated long BioLever.[24] However, this level of performance typically takes 1−2 h to attain, unlike uncoated cantilevers, which attained sub-pN stability just 30 min after mounting.[24] We emphasize that this limitation will only affect long time scale experiments. The improved short-term force precision (Figure 5) is immediately accessible and useful in a wide range of AFM-based assays. For scientists familiar with standard gold-coated cantilevers, the long-term drift of our modified cantilevers is significantly less and stabilizes on a more rapid time scale than traditional cantilevers.

CONCLUSIONS

We have developed an efficient way to fabricate soft, but short, AFM cantilevers. Their 10-fold lower β leads to better short-term force precision. Their 10-fold lower k, coupled with the removal of all of the gold except from the end of the cantilever, leads to excellent long-term force stability. The protected gold patch enables high reflectivity, without loss of such stability. Importantly, these FIB-modified cantilevers are neither too complex to fabricate nor too costly for routine use in a commercial AFM. Moreover, our work extends earlier thermal noise characterization of FIB-modified cantilevers[28,29] by directly demonstrating enhanced performance in a common single-molecule assay, the mechanical unfolding of a protein. We highlighted this improvement in three different force spectroscopy assays. First, we showed significantly improved short-term force precision during a dynamic unfolding assay (Figure 5). Second, we showed sub-pN performance over five decades of bandwidth ($\Delta f \approx$ 0.01−1000 Hz) while stretching a surface-anchored protein (Figure 6b). Finally, we showed the temporal response of the cantilever to a protein unfolding remained excellent (∼70 μs) despite the cantilever's reduced k (Figure 6d). Hence, these FIB-modified cantilevers show enhanced performance in multiple force spectroscopy assays. We expect these enhancements can immediately improve a wide range of other AFM-based studies in biophysics and nanotechnology.

METHODS

Focused Ion Beam Modification of a Commercial Cantilever. We used a dual-beam FIB (Nova NanoLab 600, FEI) that has both an electron (e) beam and an ion (Ga^{2+}) beam. The e-beam was used to write the glass-like structure, to compensate for charging during FIB-milling,[51] and to image the resulting structure. The ion-beam was used to remove material from the cantilever.

The protocol begins by loading the cantilevers into the FIB using a custom-made metal mounting plate. This mounting geometry held 9 cantilevers, which were affixed to the mounting plate with graphite tape. The graphite tape helped minimize the charging of the cantilever during FIB-modification; excess charge on insulating samples leads to degraded performance in scanning electron microscopy (SEM) and FIB applications.[51] We next loaded the sample into the FIB. It took ∼20 min to

achieve a vacuum of 10^{-5} Torr (1.3 mPa), our typical base pressure.

We used an e-beam induced deposition process[52] to form the capping layer (Figure 2b) that protected the gold during subsequent chemical etches. The mask was transparent and made from a precursor gas (TEOS, FEI). The gas was introduced into the FIB vacuum chamber through a micromanipulator-controlled needle as part of the manufacturer's gas injection system (GIS). This system allowed us to position a needle close (~400 μm) to the sample, improving gas adsorption without compromising the base pressure of the main FIB chamber. The gas flow rate was controlled by the pressure of the precursor gas, which was typically ~1 Torr (130 Pa). Gas adsorbed on the surface forms a solid glass-like material when irradiated with an e-beam of adequate energy (>1 eV). The precursor gas is more effectively activated by secondary electrons (~10 eV) than high energy electrons (10 keV), due to its larger cross section for low energy electrons. Secondary electrons (<50 eV) are efficiently produced by the e-beam as it scatters in the substrate (*i.e.*, the silicon nitride of the cantilever).[52] To do so, we used a tightly focused (~150 nm diameter) 100-pA 5 keV e-beam. Raster scanning this e-beam enabled us to generate the desired 8×12 μm^2 pattern. The pattern itself was laid out using the manufacturer's software and had a pixel size of the ~175 nm. The dwell time per pixel during the writing process was 0.04 ms. We repeated the pattern 5000 times for a total write time of 6 min. We used the e-beam limited regime for deposition, in contrast to an adsorption-limited one, to achieve better mask continuity and improved deposition purity.[52]

To remove the large, central region of the cantilever (Figure 2c), we first had to overcome a significant problem associated with FIB modification of soft cantilevers: they vibrated and/or folded back upon themselves during the milling process. The cause of these unwanted cantilever dynamics was charging of the cantilever, a problem that was partially, but not fully, alleviated by using graphite tape in the mounting process. The traditional solution to this problem is to sputter extra gold onto the cantilever,[51] an added step in handling of each cantilever. We avoided this additional step with two modifications to the FIB-milling process. The first modification was to apply a defocused e-beam (10 μm diam; 1.5 nA) to the cantilever concurrent with the FIB milling. The negative electrons helped neutralize the positive charge build up from the Ga^{2+} ions.[51] The second modification was to start the milling process on the segment of the cantilever farthest from the chip. This simple procedure preserved the inherent stiffness of the unmodified cantilever for as long as possible to resist folding or vibrating. The actual milling was accomplished using a relatively tightly focused ion beam (<300 nm diam; 100 pA) to cut the perimeter around a rectangular region. To avoid damage to the cantilever during the prolonged irradiation resulting from the focusing process,[53] we focused the ion beam on a triangular portion of the cantilever material left over from the manufacturing process that is next to the rectangular cantilever as seen in Figure 1b. After focusing, the cantilever thickness was milled through entirely in ~5 min using a 40 nm pixel spacing and a ~0.2 ms dwell times. At the completion of cutting, the rectangular section fell away, leaving two narrow supports holding the tip-containing section of the cantilever (Figure 2c).

To further reduce k, the narrow-width supports were thinned by ~30%. The primary challenge was maintaining cantilever integrity. We achieved better results when we implemented a technique using an ion beam defocused to 2 μm, a value chosen on the basis of Stokes *et al.*[51] This width was slightly wider than the full width of the support. Two potential explanations for this improved performance are (i) a larger beam size should reduce localized charging that could distort these fragile cantilevers[53] and (ii) a reduced dosage per unit area should reduce the rate of milling, making the thinning more uniform over the width of the support.[54] Once we defined this large beam size, the 100 pA beam was moved in a linear pattern along the support in a single-pixel-wide line pattern, removing the exposed top layer of material. To minimize excess milling at the turning points in the line pattern, the turning points were chosen to be outside the narrow support region, as evidenced by the lighter color gray regions shown in Figure 1c. We observed no noticeable detrimental effects of charging when moving the ion beam in a cyclic pattern repeated every ~0.5 s. We repeated this pattern a total of 500 times over 4 min.

We removed the cantilever's gold coating using a ~40 s wet etch (Type TFA, Transene) (Figure 2e). The underlying chromium adhesion layer was then removed using a ~40 s wet etch (Cr Etchent, Transene). Each etch was separated by a water bath and blotted dry using the corner of a kimwipe (Kimtech).

Characterizations of Micromachined Cantilevers. We used a commercial AFM (Cypher, Asylum Research with its standard, not small, spot size module installed) to compare the performance of the modified cantilevers to commercial ones that had their gold coating removed. For these measurements, the AFM was configured using the instrument's "crosspoint panel" to bypass the default high-pass filter, enabling accurate measurement over a broad frequency range. Cantilever stiffness was calibrated in liquid far from the surface using the instrument's built-in fitting algorithm.[55] To determine the reduction in k due to FIB modification, the stiffness of all micromachined cantilevers was measured before and after modification.

We used two primary metrics to assess cantilever performance in liquid: the integrated force noise and the Allan variance.[39] After letting each cantilever equilibrate in 150 mM phosphate buffer (pH 8) for 1−2 h, we touched the cantilever off the surface and then retracted it by 50 nm. The cantilever's thermal motion was then digitized in five 100 s segments at 50 kHz. We first calculated the positional power spectral density (PSD) and then multiplied it by the cantilever stiffness to yield the force PSD. The integrated force noise was calculated by integrating the force power spectral density (PSD) over the specified bandwidth. The Allan variance σ was calculated from the same data using

$$\sigma_x(T) = \sqrt{\frac{1}{2}\langle (x_{i+1} - x_i)^2 \rangle_T} \quad (1)$$

where T is the averaging time interval, and x_i is the mean value of the data over the ith time interval.[39] We have previously used these metrics to analyze uncoated BioLever Minis and long BioLevers.[21,24]

We used two methods to probe the hydrodynamic drag of the cantilever. The first was quite simple, but assumed overdamped motion. An overdamped oscillator displaced from equilibrium will decay exponentially toward equilibrium. The characteristic decay time is given by $\tau = \beta/k$.[41] We have experimental access to τ and k, allowing β to be computed. The stiffness calibration yielded k. We computed τ based on e^{-1} value in the autocorrelation in the cantilever's thermal motion.

The second method is based upon Stokes drag, where the cantilever was moved vertically up and down in a sawtooth pattern at varying velocities (v = 15−60 μm/s). A uniform velocity led to a constant cantilever deflection. A generalization of Stoke's law yields a phenomenological definition of hydrodynamic drag, $\beta = F/v$. From these measurements, we got a second determination of β for the three different cantilevers studied (Figure S1, SI).

Single Molecule Force Spectroscopy of a Polyprotein. To test our micromachined cantilevers in a biological assay, we studied a polyprotein of NuG2, a fast-folding variant of GB1.[42] In this construct, there are eight identical tandem repeats of the NuG2 domain, a N-terminal His-tag to facilitate purification, and an N-terminal cysteine to facilitate surface anchoring.[56] The mechanical unfolding properties of this polyprotein have been previously characterized using AFM-based SMFS.[56]

Historically, AFM-based SMFS is done by passively absorbing the protein onto a glass or mica surface and relying on nonspecific interactions between the tip and the protein. To improve the stability of the attachment for taking 100 s records, we prepared glass substrates coated with NHS-PEG-maleimide based upon prior work.[57] The PEG surface dramatically decreases the nonspecific sticking of the protein to the surface.[58] The maleimide moiety enables covalent attachment of the

NuG2 polyprotein to the surface *via* its N-terminal cysteine. We incubated 1 μL of ~500 nM NuG2 in 100 μL of 150 mM phosphate buffer (pH 8) and 1 μL of 10 mM TCEP for 1 h at room temperature and then rinsed with 400 μL of phosphate buffer. Cantilevers were illuminated with UV light for 1 min (Bondwand, Electro-Lite Corp.) immediately prior to loading to promote nonspecific attachment to the uncoated cantilever. Samples and the cantilever were loaded and equilibrated for >1 h prior to measurements. All experiments were done in 150 mM phosphate buffer with the AFM's temperature stabilized to 27 °C.

Data were recorded with a custom program written in Asylum's MacroBuilder software. We initiated nonspecific attachment of the protein to the tip by pressing the tip into the sample at 200 pN for 1 s. The stage was then retracted at v = 400 nm/s. The records were digitized at 50 kHz. About 1% of the attempts showed a sawtooth pattern consisting of 8 ruptures with a change in contour length consistent with the unfolding of a NuG2 domain ($\Delta L \approx 17.7$ nm) (Figure S2a, SI).[59] These records were selected for analysis. For display, these high-bandwidth records were boxcar-averaged and decimated to a 1 kHz data rate. To quantify the force noise during a pulling record, a short (20 nm) linear section of the 1 kHz force−extension record was fit to a WLC model. The residuals from this fit were then plotted (Figure 5c).

To test for long-term force stability, we used a real-time selection process for molecules showing unfolding of all eight domains and a strong tip-protein interaction. This selection was achieved by proceeding only with molecules that showed F > 150 pN at an extension of at least 130 nm and then rapidly reversing the direction of the stage until F = 50 pN. The stage was held stationary during subsequent 100 s while the cantilever deflection was recorded at 50 kHz. At the conclusion of the 100 s recording, we reconfirmed the presence of the biomolecule by pulling the molecule until rupture. These trials were completed on a micromachined BioLever Mini as well as on an uncoated long BioLever and a BioLever Mini.

The temporal resolution of each cantilever was monitored by looking at the force decay after the unfolding of a NuG2 domain. As above, we selected for molecules exhibiting F > 150 pN and an extension greater than 130 nm. In this assay, the stage was rapidly moved backward a precalculated fixed amount (40 nm), sufficient to decrease F to ~10 pN based on a WLC model. After waiting for 5 s, we abruptly moved the stage position until F = 70 pN. We measured the subsequent cantilever motion for 3 s at 50 kHz. If the attachment to the polyprotein did not rupture, then the process was repeated multiple times. Individual portions of records consistent with a NuG2 domain were aligned and averaged. An exponential fit to this average curve yielded the time constant of the mechanical relaxation.

A micromachined cantilever could be reused in SMFS assays over multiple days. After each use, the cantilever was rinsed in ultrapure water and then blotted dry. At a later time, the cantilever was plasma cleaned (25 SCCM O_2, 10 s, 250 W) using a standard plasma cleaner (PlasmaSTAR, Axic). Cantilevers were stored in a gel pack for later reuse.

Conflict of Interest: The authors declare no competing financial interest.

Acknowledgment. We thank G. King for useful discussions, A. Adhikari for help in preparing functionalized glass surfaces, and B. Baxley for scientific illustration. This work was supported by the National Science Foundation [DBI-0923544, Phys-1125844], and NIST. Mention of commercial products is for information only; it does not imply NIST's recommendation or endorsement. T.T.P. is a staff member of NIST's Quantum Physics Division.

Supporting Information Available: Figures showing hydrodynamic drag of cantilevers near a surface, force−extension data modeled with WLC fits, force−extension data taken with reused FIB-modified cantilevers, and comparison of Allan variance when pulling on a protein unfolding with that of an isolated cantilever. This material is available free of charge *via* the Internet at http://pubs.acs.org.

REFERENCES AND NOTES

1. Binnig, G.; Quate, C. F.; Gerber, C. Atomic Force Microscope. *Phys. Rev. Lett.* **1986**, *56*, 930–933.
2. Engel, A.; Gaub, H. E. Structure and Mechanics of Membrane Proteins. *Annu. Rev. Biochem.* **2008**, *77*, 127–148.
3. Rief, M.; Gautel, M.; Gaub, H. E. Unfolding Forces of Titin and Fibronectin Domains Directly Measured by AFM. *Adv. Exp. Med. Biol.* **2000**, *481*, 129–141.
4. Muller, D. J.; Helenius, J.; Alsteens, D.; Dufrene, Y. F. Force Probing Surfaces of Living Cells to Molecular Resolution. *Nat. Chem. Biol.* **2009**, *5*, 383–390.
5. Muller, D. J.; Dufrene, Y. F. Atomic Force Microscopy as a Multifunctional Molecular Toolbox in Nanobiotechnology. *Nat. Nanotechnol.* **2008**, *3*, 261–269.
6. Muller, D. J.; Sapra, K. T.; Scheuring, S.; Kedrov, A.; Frederix, P. L.; Fotiadis, D.; Engel, A. Single-Molecule Studies of Membrane Proteins. *Curr. Opin. Struct. Biol.* **2006**, *16*, 489–495.
7. Scheuring, S.; Sturgis, J. N. Chromatic Adaptation of Photosynthetic Membranes. *Science* **2005**, *309*, 484–487.
8. Ando, T. High-Speed Atomic Force Microscopy Coming of Age. *Nanotechnology* **2012**, *23*, 062001.
9. Fernandez, J. M.; Li, H. Force-Clamp Spectroscopy Monitors the Folding Trajectory of a Single Protein. *Science* **2004**, *303*, 1674–1678.
10. Rief, M.; Gautel, M.; Oesterhelt, F.; Fernandez, J. M.; Gaub, H. E. Reversible Unfolding of Individual Titin Immunoglobulin Domains by AFM. *Science* **1997**, *276*, 1109–1112.
11. Muller, D. J.; Schabert, F. A.; Buldt, G.; Engel, A. Imaging Purple Membranes in Aqueous Solutions at Sub-Nanometer Resolution by Atomic Force Microscopy. *Biophys. J.* **1995**, *68*, 1681–1686.
12. Schabert, F. A.; Henn, C.; Engel, A. Native *Escherichia coli* OmpF Porin Surfaces Probed by Atomic Force Microscopy. *Science* **1995**, *268*, 92–94.
13. Muller, D. J.; Fotiadis, D.; Scheuring, S.; Muller, S. A.; Engel, A. Electrostatically Balanced Subnanometer Imaging of Biological Specimens by Atomic Force Microscope. *Biophys. J.* **1999**, *76*, 1101–1111.
14. Muller, D. J.; Schoenenberger, C. A.; Schabert, F.; Engel, A. Structural Changes in Native Membrane Proteins Monitored at Subnanometer Resolution with the Atomic Force Microscope: A Review. *J. Struct. Biol.* **1997**, *119*, 149–157.
15. Junker, J. P.; Ziegler, F.; Rief, M. Ligand-Dependent Equilibrium Fluctuations of Single Calmodulin Molecules. *Science* **2009**, *323*, 633–637.
16. Rief, M.; Clausen-Schaumann, H.; Gaub, H. E. Sequence-Dependent Mechanics of Single DNA Molecules. *Nat. Struct. Biol.* **1999**, *6*, 346–349.
17. Rief, M.; Oesterhelt, F.; Heymann, B.; Gaub, H. E. Single Molecule Force Spectroscopy on Polysaccharides by Atomic Force Microscopy. *Science* **1997**, *275*, 1295–1297.
18. Muller, D. J.; Dufrene, Y. F. Atomic Force Microscopy: A Nanoscopic Window on the Cell Surface. *Trends Cell Biol.* **2011**, *21*, 461–469.
19. Dufrene, Y. F.; Evans, E.; Engel, A.; Helenius, J.; Gaub, H. E.; Muller, D. J. Five Challenges to Bringing Single-Molecule Force Spectroscopy into Living Cells. *Nat. Methods* **2011**, *8*, 123–127.
20. Casuso, I.; Scheuring, S. Automated Setpoint Adjustment for Biological Contact Mode Atomic Force Microscopy Imaging. *Nanotechnology* **2010**, *21*, 035104.
21. Sullan, R. M.; Churnside, A. B.; Nguyen, D. M.; Bull, M. S.; Perkins, T. T. Atomic Force Microscopy with Sub-PicoNewton Force Stability for Biological Applications. *Methods* **2013**, *60*, 131–141.
22. Liphardt, J.; Onoa, B.; Smith, S. B.; Tinoco, I. J.; Bustamante, C. Reversible Unfolding of Single RNA Molecules by Mechanical Force. *Science* **2001**, *292*, 733–737.
23. Viani, M. B.; Schaffer, T. E.; Chand, A.; Rief, M.; Gaub, H. E.; Hansma, P. K. Small Cantilevers for Force Spectroscopy of Single Molecules. *J. Appl. Phys.* **1999**, *86*, 2258–2262.
24. Churnside, A. B.; Sullan, R. M.; Nguyen, D. M.; Case, S. O.; Bull, M. S.; King, G. M.; Perkins, T. T. Routine and Timely Sub-picoNewton Force Stability and Precision for Biological

Applications of Atomic Force Microscopy. *Nano Lett.* **2012**, *12*, 3557–3561.
25. King, G. M.; Carter, A. R.; Churnside, A. B.; Eberle, L. S.; Perkins, T. T. Ultrastable Atomic Force Microscopy: Atomic-Scale Lateral Stability and Registration in Ambient Conditions. *Nano Lett.* **2009**, *9*, 1451–1456.
26. Zocher, M.; Roos, C.; Wegmann, S.; Bosshart, P. D.; Dotsch, V.; Bernhard, F.; Muller, D. J. Single-Molecule Force Spectroscopy from Nanodiscs: An Assay to Quantify Folding, Stability, and Interactions of Native Membrane Proteins. *ACS Nano* **2012**, *6*, 961–971.
27. Sapra, K. T.; Besir, H.; Oesterhelt, D.; Muller, D. J. Characterizing Molecular Interactions in Different Bacteriorhodopsin Assemblies by Single-Molecule Force Spectroscopy. *J. Mol. Biol.* **2006**, *355*, 640–650.
28. Maali, A.; Cohen-Bouhacina, T.; Jai, C.; Hurth, C.; Boisgard, R.; Aime, J. P.; Mariolle, D.; Bertin, F. Reduction of the Cantilever Hydrodynamic Damping Near a Surface by Ion-Beam Milling. *J. Appl. Phys.* **2006**, *99*, 024906.
29. Hodges, A. R.; Bussmann, K. M.; Hoh, J. H. Improved Atomic Force Microscope Cantilever Performance by Ion Beam Modification. *Rev. Sci. Instrum.* **2001**, *72*, 3880–3883.
30. Noy, A.; Vezenov, D. V.; Kayyem, J. F.; Meade, T. J.; Lieber, C. M. Stretching and Breaking Duplex DNA by Chemical Force Microscopy. *Chem. Biol.* **1997**, *4*, 519–527.
31. Denis, F. A.; Hanarp, P.; Sutherland, D. S.; Gold, J.; Mustin, C.; Rouxhet, P. G.; Dufrene, Y. F. Protein Adsorption on Model Surfaces with Controlled Nanotopography and Chemistry. *Langmuir* **2002**, *18*, 819–828.
32. Piner, R. D.; Zhu, J.; Xu, F.; Hong, S.; Mirkin, C. A. "Dip-Pen" Nanolithography. *Science* **1999**, *283*, 661–663.
33. Liu, M. Z.; Amro, N. A.; Chow, C. S.; Liu, G. Y. Production of Nanostructures of DNA on Surfaces. *Nano Lett.* **2002**, *2*, 863–867.
34. Labuda, A.; Bates, J. R.; Grütter, P. H. The Noise of Coated Cantilevers. *Nanotechnology* **2012**, *23*, 025503.
35. Svoboda, K.; Block, S. M. Biological Applications of Optical Forces. *Annu. Rev. Biophys. Biomol. Struct.* **1994**, *23*, 247–285.
36. Kawakami, M.; Taniguchi, Y.; Hiratsuka, Y.; Shimoike, M.; Smith, D. A. Reduction of the Damping on an AFM Cantilever in Fluid by the Use of Micropillars. *Langmuir* **2010**, *26*, 1002–1007.
37. Yu, H.; Liu, X.; Neupane, K.; Gupta, A. N.; Brigley, A. M.; Solanki, A.; Sosova, I.; Woodside, M. T. Direct Observation of Multiple Misfolding Pathways in a Single Prion Protein Molecule. *Proc. Natl. Acad. Sci. U. S. A.* **2012**, *109*, 5283–5288.
38. Stigler, J.; Ziegler, F.; Gieseke, A.; Gebhardt, J. C. M.; Rief, M. The Complex Folding Network of Single Calmodulin Molecules. *Science* **2011**, *334*, 512–516.
39. Sullivan, D. B.; Allan, D. W.; Howe, D. A.; Walls, E. L. *Characterization of Clocks and Oscillators*; U.S. Government Printing Office: Washington, D.C., 1990.
40. Czerwinski, F.; Richardson, A. C.; Oddershede, L. B. Quantifying Noise in Optical Tweezers by Allan Variance. *Opt. Express* **2009**, *17*, 13255–13269.
41. Howard, J. *Mechanics of Motor Proteins and the Cytoskeleton*; Sinauer Associates: Sunderland, MA, 2001.
42. Nauli, S.; Kuhlman, B.; Baker, D. Computer-Based Redesign of a Protein Folding Pathway. *Nat. Struct. Biol.* **2001**, *8*, 602–605.
43. Janovjak, H.; Struckmeier, J.; Muller, D. J. Hydrodynamic Effects in Fast AFM Single-Molecule Force Measurements. *Eur. Biophys. J.* **2005**, *34*, 91–96.
44. Liu, R. C.; Roman, M.; Yang, G. L. Correction of the Viscous Drag Induced Errors in Macromolecular Manipulation Experiments Using Atomic Force Microscope. *Rev. Sci. Instrum.* **2010**, *81*, 063703.
45. Rico, F.; Gonzalez, L.; Casuso, I.; Puig-Vidal, M.; Scheuring, S. High-Speed Force Spectroscopy Unfolds Titin at the Velocity of Molecular Dynamics Simulations. *Science* **2013**, *342*, 741–743.
46. Dufrene, Y. F.; Martinez-Martin, D.; Medalsy, I.; Alsteens, D.; Muller, D. J. Multiparametric Imaging of Biological Systems by Force-Distance Curve-Based AFM. *Nat. Methods* **2013**, *10*, 847–854.
47. Alsteens, D.; Dupres, V.; Yunus, S.; Latge, J. P.; Heinisch, J. J.; Dufrene, Y. F. High-Resolution Imaging of Chemical and Biological Sites on Living Cells using Peak Force Tapping Atomic Force Microscopy. *Langmuir* **2012**, *28*, 16738–16744.
48. Medalsy, I.; Hensen, U.; Muller, D. J. Imaging and Quantifying Chemical and Physical Properties of Native Proteins at Molecular Resolution by Force-Volume AFM. *Angew. Chem., Int. Ed.* **2011**, *50*, 12103–12108.
49. Rico, F.; Su, C. M.; Scheuring, S. Mechanical Mapping of Single Membrane Proteins at Submolecular Resolution. *Nano Lett.* **2011**, *11*, 3983–3986.
50. Cecconi, C.; Shank, E. A.; Bustamante, C.; Marqusee, S. Direct Observation of the Three-State Folding of a Single Protein Molecule. *Science* **2005**, *309*, 2057–2060.
51. Stokes, D. J.; Vystavel, T.; Morrissey, F. Focused Ion Beam (FIB) milling of Electrically Insulating Specimens Using Simultaneous Primary Electron and Ion Beam Irradiation. *J. Phys. D: Appl. Phys.* **2007**, *40*, 874–877.
52. van Dorp, W. F.; Hagen, C. W. A Critical Literature Review of Focused Electron Beam Induced Deposition. *J. Appl. Phys.* **2008**, *104*, 081301.
53. Giannuzzi, L. A.; Stevie, F. A. *Introduction to Focused Ion Beams: Instrumentation, Theory, Techniques and Practice*; Springer: New York, 2005.
54. Hopman, W. C. L.; Ay, F.; Hu, W. B.; Gadgil, V. J.; Kuipers, L.; Pollnau, M.; de Ridder, R. M. Focused Ion Beam Scan Routine, Dwell Time and Dose Optimizations for Submicrometre Period Planar Photonic Crystal Components and Stamps in Silicon. *Nanotechnology* **2007**, *18*, 195305.
55. Proksch, R.; Schaffer, T. E.; Cleveland, J. P.; Callahan, R. C.; Viani, M. B. Finite Optical Spot Size and Position Corrections in Thermal Spring Constant Calibration. *Nanotechnology* **2004**, *15*, 1344–1350.
56. Cao, Y.; Kuske, R.; Li, H. Direct Observation of Markovian Behavior of the Mechanical Unfolding of Individual Proteins. *Biophys. J.* **2008**, *95*, 782–788.
57. Zimmermann, J. L.; Nicolaus, T.; Neuert, G.; Blank, K. Thiol-Based, Site-Specific and Covalent Immobilization of Biomolecules for Single-Molecule Experiments. *Nat. Protoc.* **2010**, *5*, 975–985.
58. Ha, T.; Rasnik, I.; Cheng, W.; Babcock, H. P.; Gauss, G. H.; Lohman, T. M.; Chu, S. Initiation and Re-Initiation of DNA Unwinding by the *Escherichia coli* Rep Helicase. *Nature* **2002**, *419*, 638–641.
59. Cao, Y.; Balamurali, M. M.; Sharma, D.; Li, H. B. A Functional Single-Molecule Binding Assay *via* Force Spectroscopy. *Proc. Natl. Acad. Sci. U. S. A.* **2007**, *104*, 15677–15681.